[type=editor, auid=000,bioid=1, prefix=MSc, role=developer inventor, orcid=0000-0002-0282-0972]

Highlights

Multiple Sensor Interface by the same hardware to USB and serial connection

David Nuno Quelhas

- multiple sensor interface using same hardware to serial connection

- measurement of sensors based on resistance, capacitance, inductance, frequency

- versatile electronics for basic measurement requirements (or low-end usage)

- electronics design aiming for reuse, repurpose, repair, customization

Multiple Sensor Interface by the same hardware to USB and serial connection

David Nuno Quelhas[a,a]

[a]*Lisboa, Portugal*

Abstract

The Multiple Sensor Interface is a simple sensor interface that works with USB, RS485 and GPIO. It allows one to make measurements using a variety of sensors based on the change of inductance, resistance, capacitance, and frequency using the same connector and same electronic interface circuit between the sensor and the microcontroller. The same device also provides some additional connectors for small voltage measurement. Any sensors used for the measurement of distinct phenomena can be used if the sensor output is based on inductance, resistance, capacitance or frequency within the measurement range of the device, obtaining a variable precision depending on the used sensor. The device presented is not meant for precise or accurate measurements. It is meant to be a reusable hardware that can be adapted/configured to a varied number of distinct situations, providing, to the user, more freedom in sensor selection as well as more options for device/system maintenance or reuse.

Keywords:
Computer peripherals, Oscillators, Sensor systems and applications, Signal processing

1. Introduction

The electronic waste (e-waste) is a modern problem under increasing concern and awareness, there are various possible approaches to reduce and mitigate it, most obvious is the collection and recycling of discarded devices, however the most ideal was just to design and produce technology that lasts because not only is physically fit by quality design, production, and components; but because its design was intended to be most versatile ensuring the same device can be used and reused in various applications/contexts just by changing connections, jumpers, and firmware configurations. Some design aspects for making a device more reusable are: use of standard connectors and protocols, think of it as a module to be part of a larger system, minimize barriers for connecting/interfacing components and devices from distinct manufacturers.

1.1. Project objectives and trade-offs

-This article will focus on the design of a sensor interface device with USB and serial(UART,RS-485), aimed to allow interface to many distinct 2-wire sensors based on the change of inductance, resistance, capacitance, frequency, and also small voltage; sensors that can be interchanged using the same hardware and same port of the device, thus meaning the electronics designed must also be versatile.

-Obviously providing a versatile device to the users will have its negative trade-offs, like: 1- probably significant lower precision/accuracy, 2- some sensor calibration must be provided/done by the end user after replacing a sensor, 3- the calibration function will not be linear or 'easy' as desired for sensors and its interfaces.

-However for some applications the mentioned trade-offs are not necessarily a deal-breaker, like when the user is technical and is ok with using a device that requires more setup/configuration, some users like devices that are more customizable or repairable. Also a device that if no longer useful for a user, it might still be useful for another user on a different application/context.

1.2. License and context

- The hardware design here disclosed is distributed under "CERN Open Hardware Licence Version 2 - Weakly Reciprocal" (CERN-OHL-W), its associated software/firmware under GNU licenses (GPL, LGPL).

- This article is published under the Creative Commons license CC BY-NC-SA 4.0 (Attribution-NonCommercial-ShareAlike 4.0 International).

- This article is about a 'hobby' project done by the author (David Nuno Quelhas, MSc Electronics Eng, alumni of Instituto Superior Tecnico, Portugal) with occasional 'work' between years 2012 and 2021 on his 'free time'.

1.3. State of the art

- The purpose of this article is to disclose a design aimed to be most versatile possible, and so not focused on a specific application type or use; and since the author doesn't know of other articles focused on a most versatile/reusable/repairable design to same type of device; the author did not find meaningful to mention other articles or designs as state of the art or to make comparisons.

Email address: `david.n.quelhas@gmail.com` (David Nuno Quelhas)

URL: `https://pt.linkedin.com/in/dquelhas` (David Nuno Quelhas), `https://multiple-sensor-interface.blogspot.com` (David Nuno Quelhas)
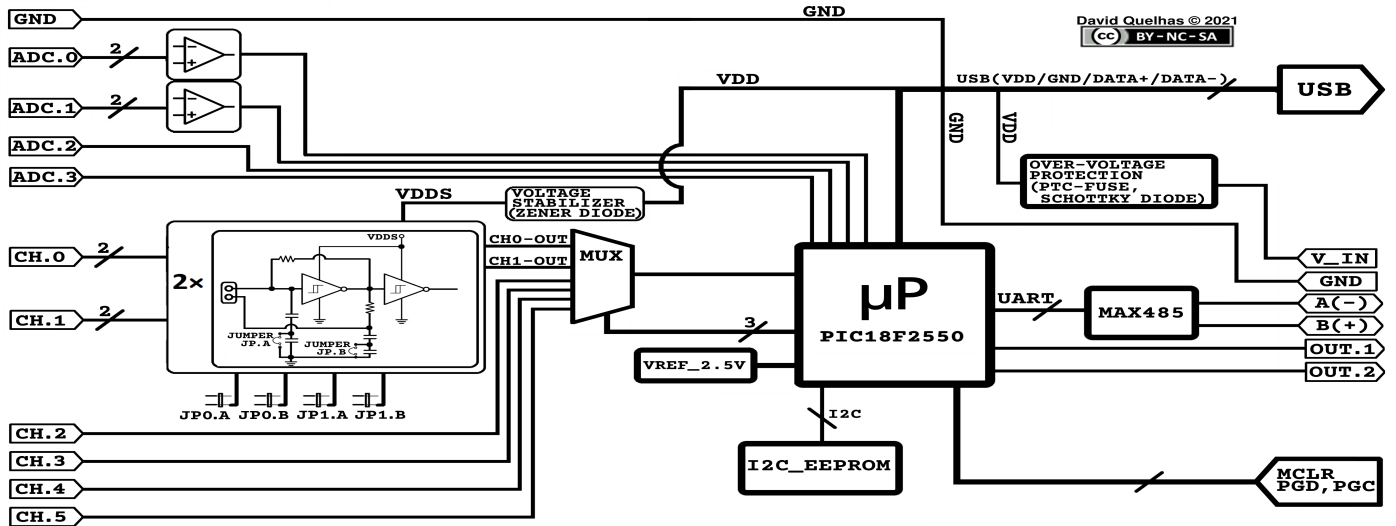
Figure 1: Diagram of the Multiple Sensor Interface device.

2. Sensor Interface Device

Here is presented the Multiple Sensor Interface, the interface main components/sub-circuits are: The connectors and sensor interface circuits (oscillators) for inductance, resistance, capacitance and frequency (CH.0, CH.1); the connectors and over-voltage protection(zener diode) for frequency measurement (CH.2, CH.3, CH.4, CH.5); the connectors and interface circuit for voltage measurement (ADC.0, ADC.1, ADC.2, ADC.3); analog multiplexer for the sensor channels, the microprocessor(PIC18F2550); I2C EEPROM for storing calibration tables; USB connector; serial connector and circuit for RS-485 and UART; digital outputs connector (OUT.1, OUT.2).

The digital outputs have the value of a boolean function defined by the user, boolean functions with logic variables that are the result of a comparison ('bigger' or 'smaller' than), between the value/measurement of a sensor channel and a configurable threshold value.

The connectors used for frequency measurement may be connected to external single sensor interface circuits (oscillators).

2.1. The sensor interface circuit (oscillator)

The sensor interface circuit is an oscillator, with its design based on the Pierce oscillator, however are some modifications to the Pierce oscillator, the 1st difference is that there is no quartz crystal, and on the location of the crystal will be connected the sensor to be measured (variable inductance or resistance or capacitance), the 2nd difference is that instead of simple inverters ('NOT' gates) will be used Schmitt-trigger inverters(high-speed Si-gate CMOS, 74HC14) this is a very relevant difference that will allow the oscillator to work even with a resistive or capacitive sensor (in fact the oscillator circuit is two different oscillator types depending on the sensor connected by the user), also the use of Schmitt-Trigger inverters will minimize signal jitter of the oscillator output.

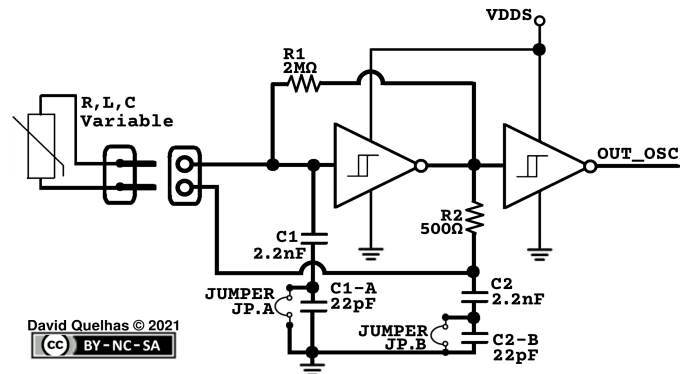- The sensor interface circuit has 2 pairs of series ca-

Figure 2: Schematic of the sensor interface circuit (oscillator).

pacitors (C1 2.2nF,C1-A 22pF and C2 2.2nF,C2-B 22pF) instead of just 2 capacitors(C1,C2) so the value of C1 and C2 can be adjusted just by placing/removing a jumper; placing a jumper removes C1-A or C1-B from the circuit making 2.2nF the value of C1 or C2; removing the jumper lets the capacitors in series making 21.78pF the total value of (C1, C1-A) or (C2, C2-B). So on the rest of the article, whenever is mentioned C1 or C2 is meant the resulting capacitor value that can be 2.2nF(jumper on) or 21.78pF(jumper off), accordingly with mentioned jumper configuration.

- The sensors can be connected directly on the Multiple-Sensor Interface (on then screw terminals/connectors), or by using a cable, in case the cable is longer than 20cm is recommended the used of shielded twisted-pair (STP) cable to prevent cross-talk between sensor channels or external EMI.

3. Measurement process

The Multiple-Sensor device has a microprocessor (PIC18F2550) that is able to make frequency and voltage measurements, so the device will make frequency measurements for sensor channels CH.0 to CH.5 ; and will make voltage measurements for sensor channels (ADC.0 to ADC.3); these frequency and voltage measurements made

2

by the device will be designated as the RAW_value of a sensor channel. To obtain the measurement of a sensor channel the device will then use a 2 column calibration table that is a long list of points (RAW_value; measurement) relating the measurement value (obtained during calibration by an external reference device) to the corresponding RAW_value obtained on the Multiple-Sensor device, these calibration tables will be stored on an I2C EEPROM memory on the Multiple-Sensor device.

-The Multiple-Sensor device can work in two modes: single-channel or multiple-channel, the CH.0 to CH.5 RAW_value(frequency) will be calculated through a counter/timer of the PIC18F2550 by periodically reading its value and calculating the frequency f[Hz]=count[cycles]/period[s]. So in single-channel mode the frequency will be always calculated on the selected/enabled sensor channel, in multiple-sensor mode the frequency will be calculated for each sensor channel sequentially (time-division multiplexing) since there are 6 channels to measure but only on counter/timer of the microprocessor for that job. Thus in multiple-channel mode the measurement will take 6x more time to be updated/refreshed than in single-channel mode.

-For the sensor channels ADC.0 to ADC.3 the RAW_value is the voltage of those channels measured by using the ADC (Analog to Digital Converter) of the microprocessor and also reading a 2.5V voltage reference.

-The sensor measurements will be calculated by searching the RAW_value on the correspondent calibration table, and will be used from the table 2 points (RAW_value,measurement) referenced here as points A and B such that the measured RAW_value is bigger than RAW_value of A and is lower than RAW_value of B; then will be calculated a linear equation: $measurement=a\cdot(\text{RAW\_value}) + b$ defined by the points A and B; and so every-time the device calculates a sensor measurement it will calculate the correspondent linear equation for the current RAW_value and use it to obtain the current measurement (Fig. 3) .
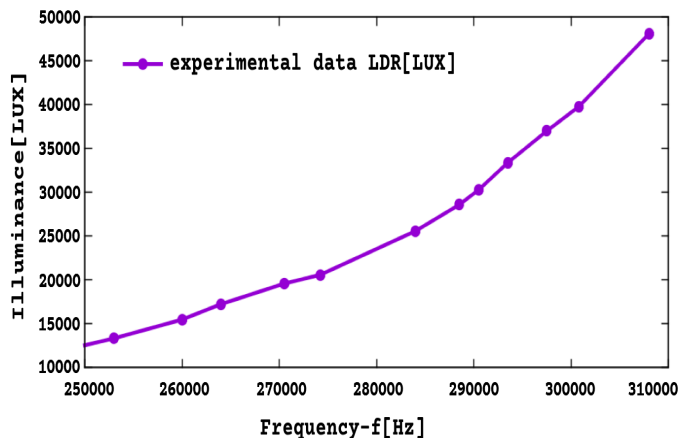
Figure 3: Plot experimental data with line, LDR light(brightness) sensor connected on Multiple-Sensor Interface; example of a calibration table exclusively from experimental data.
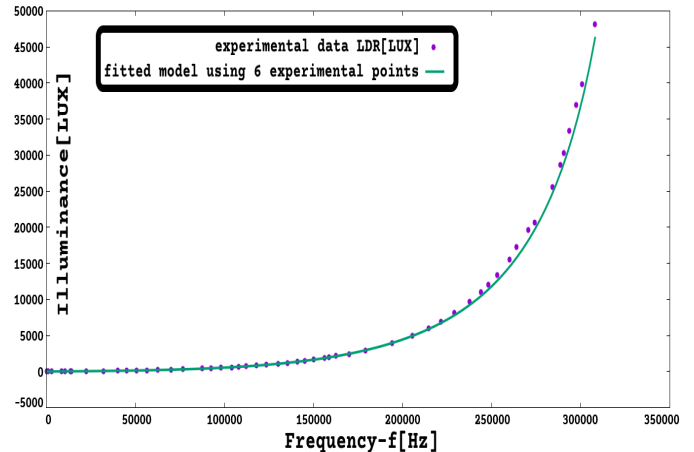
Figure 4: Plot experimental data and fitted model, LDR light(brightness) sensor connected on Multiple-Sensor Interface; model fit by using 6 points of experimental data.

3.1. Device calibration for a sensor

-So device calibration is about obtaining calibration tables for each sensor channel, there are 2 ways to obtain a calibration table:

1- Do a full manual calibration using an external meter as reference where both the reference meter and the Multiple-sensor device(with a sensor connected) are exposed to same stimulus/environment that is controllable by the user to produce all adequate variations/intensities necessary to record an extensive calibration table, with all experimental pairs of (RAW_value,measurement).

2- Using a know function that relates the measured phenomena to the obtained RAW_value on the Multiple-Sensor device (obtained by theoretical or experimental study), although a purely theoretical calibration could be used, probably is better or easier to obtain a calibration table by using a known function and have its constants/parameters calculated by a data fitting to some few experimental data points (RAW_value, measurement) obtained for the device calibration. So for example if the know function had 6 constants/parameters you would require at least 6 different experimental measurements to obtain the function for that sensor channel, then having the function is just a question calculating a longer list of pairs (RAW_value,measurement) on the desired measurement range. The (Fig. 4) is the result of fitting the model function $Illuminance(f) = (a + (b/(c + d\cdot f)))\cdot((n\cdot f^2) + m)$ to the points (229Hz, 0LUX; 8500Hz, 10LUX; 14000Hz, 30LUX; 76500Hz, 300LUX; 130000Hz, 1072LUX; 194000Hz, 3950LUX).

4. Sensor Interface Circuit Analysis
4.1. Multiple-Sensor Interface for Inductive sensors

When connecting an inductor or inductive sensor(having as output a change of inductance) the Multiple-Sensor Interface (Fig.2) will work as a Pierce Oscillator(where the sensor is connected instead of a quartz crystal). The theoretical analysis used here for the oscillator will be based on a model of 2 circuit blocks named 'A' and 'β' connected for feedback by connecting the output of one to the input
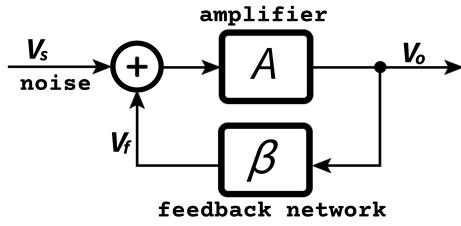
Figure 5: Diagram of model for the oscillator with an inductive sensor (Pierce Oscillator, model of feedback linear oscillator).
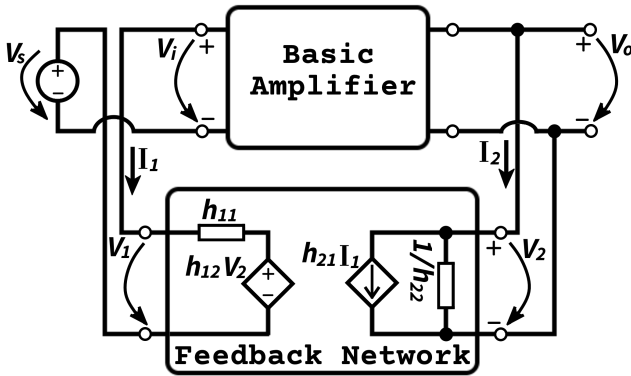

Figure 6: Representation of oscillator circuit by the h-parameters for feedback circuit (Pierce Oscillator).

other. The 'A' is an electronic amplifier providing voltage gain, the 'β' is an electronic filter providing frequency selection (resonance), so whatever voltage signal amplified by 'A' is frequency selected by 'β' and feed back to the input of A for further amplification. As know this oscillator is start-up by whatever noise available at the input of 'A', figure 5 is a diagram depicting this concept.

- The analysis of the oscillator with an inductive sensor will be made using the Barkhausen stability criterion, that says $A\beta = 1$ to be possible to occur sustained oscillations (oscillations on steady state analysis). The purpose/focus is to obtain the inductance(of sensor) as function of oscillation frequency, although most of the circuit analysis strategy used here will be similar as used for typical Pierce Oscillator with piezoelectric crystal, as available on the bibliography list "Crystal Oscillators for Digital Electronics" class notes by Peter McLean [2]. This mathematical expression simply says that a circuit with a feedback loop after reaching the steady-state is expected that any voltage signal (for example Vo) will remain steady. So from $A\beta = 1$ results: $|A\beta| = 1$ and $\angle A\beta = \pm n2\pi$.

- Starting the analysis using a possible representation of the mentioned circuit having the 'feedback network' represented by its hybrid parameters (h-parameters of a 2-port network).[1] [2]

- The Schmitt-Trigger Inverter(high-speed Si-gate CMOS) and resistors R_1, R_2 belong to circuit block 'A', the capacitors C_1, C_2 and inductive sensor L_{sensor} belong to circuit block β.

- Since the 'Basic Amplifier' has a very big input resistance the current I_1 will be very small (the electric current on the input of the inverter (CMOS 'NOT' gate) is negligible), so by using the h-parameters to represent the feed-
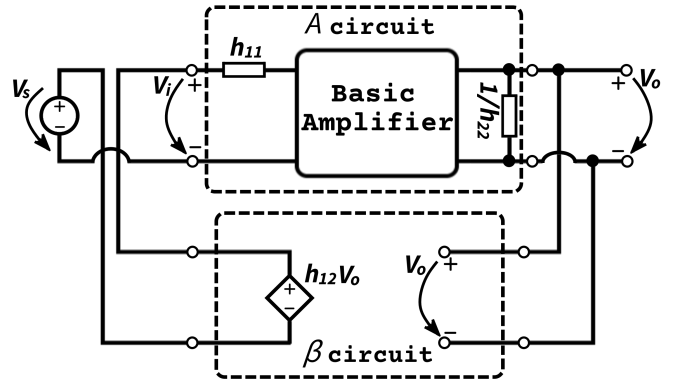

Figure 7: Simplified representation of oscillator circuit (Pierce Oscillator).
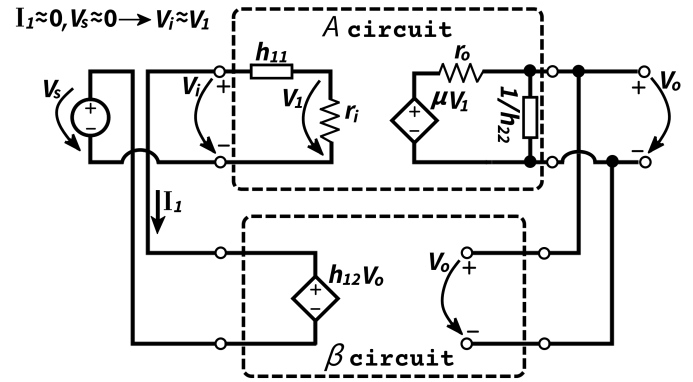

Figure 8: More simplified representation of oscillator circuit (Pierce Osc.).

back circuit block is possible to make the following simplifications/approximations: 1- The current source $h_{21}I_1$ is also negligible (equal to zero, so removed from circuit); 2- The voltage drop across component h_{11} is negligible (since $V_{11} = h_{11}I_1$, $I_1 \to 0 \Rightarrow V_{11} \to 0$) and so h_{11} can be relocated to inside the circuit block 'A' keeping V_i as the name for the voltage drop on the input of 'A' block; 3- The h_{22} can be relocated to inside the circuit block 'A' since is connected in parallel to the input of 'β' block that is also the output of 'A' block. [2]

- The block 'Basic Amplifier' is then replaced by its Thevenin equivalent circuit, obtaining the circuit on Fig-8. From this circuit you can write the transfer function (Laplace transform) of 'A' block ($V_o = AV_i$, $1/h_{22} = h_{22}^{-1}$) and 'β' block ($V_1 = \beta V_2$):

$$A = \frac{h_{22}^{-1}}{h_{22}^{-1}+r_o}\mu\frac{r_i}{r_i+h_{11}} \qquad \beta = h_{12}$$

- The feedback network (the same network displayed on Fig-6 represented by h-parameters) is the frequency-selecting π(shaped)-network on Fig-9, where Z_1, Z_2, Z_s are respectively C_1,C_2,L_{sensor} of the Multiple Sensor Interface with an inductive sensor (Pierce oscillator).

- Based on the circuit of the feedback network and using the definitions of h-parameters of a 2-port network are obtained the values:

$$h_{11} = Z_1||Z_s \qquad h_{22}^{-1} = Z_2||(Z_1+Z_s) \qquad h_{12} = \frac{Z_1}{Z_1+Z_s}$$

(where $||$ is the impedance of 2 components in parallel, $Z_1||Z_2 = (Z_1 Z_2)/(Z_1 + Z_2)$; $h_{11} = (V_1/I_1)|_{V_2=0}$; $h_{12} = (V_1/V_2)|_{I_1=0}$; $h_{22} = (I_2/V_2)|_{I_1=0}$) .
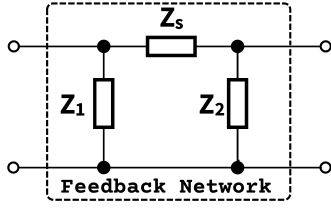
4

Figure 9: Feedback network of oscillator (Pierce Oscillator, Multiple-Sensor Interface with inductive sensor).

Finally:

$$A = \frac{Z_2||(Z_1+Z_s)}{Z_2||(Z_1+Z_s)+r_i}\mu\frac{r_i}{r_i+(Z_1||Z_s)} \qquad \beta = \frac{Z_1}{Z_1+Z_s}$$

- In the circuit of Pierce oscillator (Fig-2) the amplifier was made by a gate inverter (CMOS 'NOT' gate) and a feedback resistor ($R_1 = 2M\Omega$) biasing the inverter in its linear region of operation causing it to function as a high-gain inverting amplifier. The input resistance of CMOS 'NOT' gate is very large and so making the approximation $r_i = +\infty$ the expression of 'A' is significantly simplified, So obtaining: [2]

$$A\beta = \left(\frac{Z_2||(Z_1+Z_s)}{Z_2||(Z_1+Z_s)+r_o}\mu\right)\left(\frac{Z_1}{Z_1+Z_s}\right)$$
$$= \frac{Z_1Z_2\mu}{Z_2(Z_1+Z_s)+r_o(Z_1+Z_2+Z_s)} \quad (1)$$

- If Z_1, Z_2, Z_s are purely reactive impedances given by $Z_1 = jX_1$, $Z_2 = jX_2$, $Z_s = jX_s$ ($j = \sqrt{-1}$), then Eq-1 becomes:

$$A\beta = \frac{X_1X_2\mu}{X_2(X_1+X_s)-jr_o(X_1+X_2+X_s)} \quad (2)$$

- The Barkhausen criterion states $A\beta = 1 \rightarrow \angle A\beta = \pm n2\pi$, this means the phase shift of the loop '$A\beta$' must be zero, and so that implies that the imaginary part of Eq-2 must be zero. That is, for stable oscillations on the circuit of Fig-6 with a Feedback Network of Fig-9, it must be assured: [2]

$$X_1(\omega_0) + X_2(\omega_0) + X_s(\omega_0) = 0 \quad (3)$$

- At the frequency ω_0 (frequency of oscillation at steady state), using Eq-3 with Eq-2, is obtained: [2]

$$A(\omega_0)\beta(\omega_0) = -\mu\frac{X_1(\omega_0)}{X_2(\omega_0)} \quad (4)$$

- To start the oscillations the loop gain must be grater than unity (during Transient Response), but after achieving the Steady State Response on the Pierce oscillator for oscillations to occur the loop gain $A(\omega_0)\beta(\omega_0)$ of Eq-4 must be equal to unity('1'). Since the amplifier is an inverter ('NOT' gate with R1 feedback resistor) then μ is a negative number, and so $X_1(\omega_0)$ and $X_2(\omega_0)$ must have the same sign (both positive or negative).

- Thus, if $Z_1(\omega_0)$ is capacitive($X_1(\omega_0) = -1/(\omega_0 C_1)$), then by Eq-4 $Z_2(\omega_0)$ must also be capacitive (($X_2(\omega_0) = -1/(\omega_0 C_2)$). [2]

- Considering this and using Eq-3 its possible to conclude that $Z_s(\omega_0)$ must be inductive since $X_s(\omega_0) = -X_1(\omega_0) - X_2(\omega_0)$, this is if $X_1(\omega_0)$ and $X_2(\omega_0)$ are negative numbers then $X_s(\omega_0)$ must be a positive number, then $X_s = \omega_0 L_s$.

- So having C_1, C_2, L_s on the feedback network (where L_s is the component representing the inductive sensor on
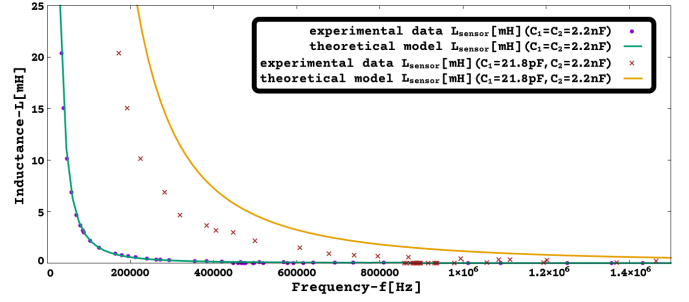

Figure 10: $L_s(f)$[mH]([Hz]) with $C_1=C_2=2.2$nF and $C_1=21.78$pF, $C_2=2.2$nF (Pierce Oscillator, Multiple-Sensor Int. with inductive sensor).
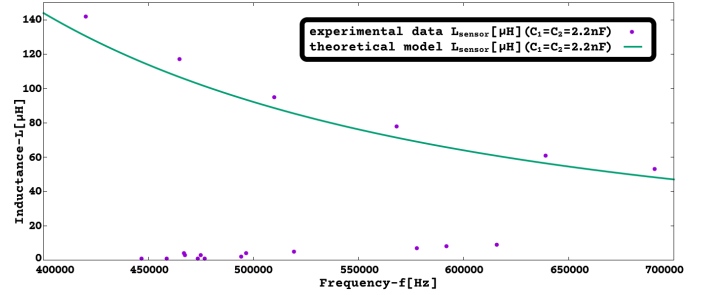

Figure 11: Frequency jump of $L_s(f)[\mu H]$([Hz]) with $C_1=C_2=2.2$nF (Pierce Oscillator, Multiple-Sensor Int. with inductive sensor).

the Multipl-Sensor Interface) the Eq-3 becomes:

$$-\frac{1}{\omega_0 C_1} - \frac{1}{\omega_0 C_2} + \omega_0 L_s = 0 \quad (5)$$

- So defining "load capacitance" C_L as: [2]

$$\frac{1}{C_L} = \frac{1}{C_1} + \frac{1}{C_2} \quad (6)$$

The frequency of oscilation on the Pierce oscillator (using C_1, C_2, L_s) is:

$$\omega_0 = \frac{1}{\sqrt{L_s C_L}} \qquad \Leftrightarrow \qquad f_0 = \frac{1}{2\pi\sqrt{L_s C_L}} \quad (7)$$

- So the expression (theoretical) of measured inductance L_{sensor} as a function of frequency(f) is:

$$L_{sensor} = L_s = \frac{1}{4\pi^2 C_L f^2} = \frac{C_1+C_2}{4\pi^2 C_1 C_2 f^2} \quad (8)$$

- On experimental tests done was observed that when using $C_1=C_2=2.2$nF (JPA and JPB closed) or when using $C_1=21.78$pF (JPA closed), $C_2=2.2$nF (JPB open), with decreasing values of L_s connected, the oscillation frequency will exhibit a sudden change, at some small value of L(around $10\mu H$ for $C_1=C_2=2.2$nF), not coherent with theoretical model of Pierce oscillator. This may be related to the fact the same circuit also implements a Schmitt-Trigger relaxation oscillator(next chapter), that will oscillate under different criteria (not related to inductance), so the author opinion is when L_s approaches some small value it may change from Pierce oscillator to Schmitt-Trigger oscillator.

- Fig-10 and Fig-11 shows the experimental data of Multiple-Sensor Interface with various inductance values connected as the sensor, also shows the plot of $L_s(f)$ using Eq-8 with $C_1=C_2=2.2$nF and $C_1=21.78$pF, $C_2=2.2$nF.

- Since the previously mentioned sudden change of the oscillator mode and frequency is not adequate on a $L_s(f)$ function usable for sensor interfacing; then on experi-
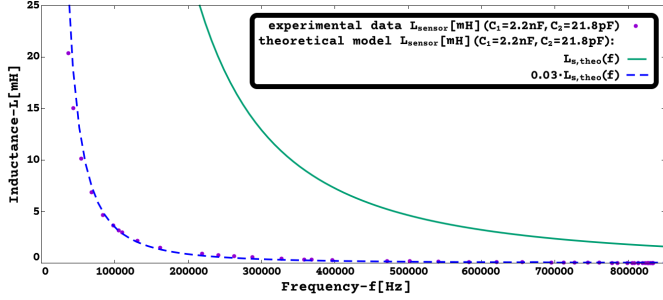
5

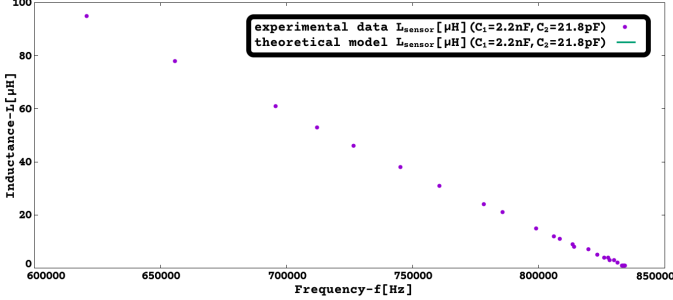Figure 12: $L_s(f)$[mH]([Hz]) with C_1=2.2nF, C_2=21.78pF (Multiple-Sensor Int. with inductive sensor).

Figure 13: Experimental data of L_s in $[0\mu H; 100\mu H]$, with C_1=2.2nF, C_2=21.78pF(Multiple-Sensor with inductive sensor).

mental tests with jumper configuration: JP.A closed and JP.B open, obtaining C_1=2.2nF and C_2=21.78pF$\approx$22nF; it was observed a continuous and progressive $f(L_s)$ function. With C_1=2.2nF and C_2=21.78pF the experimental $L_{s,expr}(f)$ followed a straight line for L_s in $[0\mu H; 100\mu H]$, then for L_s>$100\mu H$ the experimental $L_{s,expr}(f)$ continued with a shape similar to theoretical, but with different L_s values related by a constant multiplicative factor ($L_{s,expr}(f) \approx 0.03 \cdot L_{s,theo}(f)$).

- It would be expected by Eq-8, that jumper configuration with C_1=21.78pF, C_2=2.2nF and with C_1=2.2nF, C_2=21.78pF, would have the same $L_s(f)$, however experimental data shows these 2 jumper configurations have very relevant differences on $L_s(f)$, and although the author does not have a theoretical explanation for this aspect; it still was shown the device is suitable to interface inductive sensors, since with C_1=2.2nF, C_2=21.78pF it was observed a plot of $L_s(f)$ with similarities to what theory predicted, while also is suitable to generate a calibration table (frequency[Hz], measurement[μH]).

4.2. Multiple-Sensor Interface for Resistive sensors

- In case you connect a resistive sensor (or capacitive) to the Multiple-Sensor Interface you will not be able to satisfy the conditions for oscillation (Eq-3 and Eq-4) were $A(\omega_0)\beta(\omega_0)$=1, consequent of the Barkhausen criterion applied to the circuit of Multiple-Sensor Interface, as it was explained on the previous section that on the π(shaped)-network of Fig-9 if Z_1 and Z_2 are capacitive (corresponding to C_1 and C_2 of the Multiple-Sensor Interface) then Z_s must be inductive so that $A(\omega_0)\beta(\omega_0)$=1.

- So the conclusion is when you connect a resistive sensor (or capacitive) you no longer have a Pierce Oscillator, but that is not a problem because the Multiple-Sensor Interface is made using Schmitt-trigger inverters(high-speed Si-
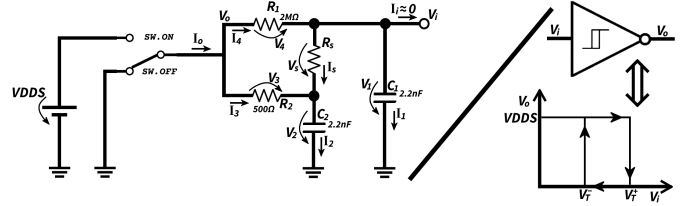

Figure 14: Multiple-Sensor Interface with resistive sensor (Schmitt-trigger inverter oscillator).

gate CMOS, 74HC14), and the Schmitt trigger is a bistable multivibrator that can be used to implement another type of multivibrator, the relaxation oscillator. So in the case of a resistive (or capacitve) sensor the circuit to analyze will be a Schmitt-trigger inverter connected to a network of resistors and capacitors.

- So to analyze this circuit the Schmitt-trigger inverter will be replaced by a theoretical switch that will change the voltage of node v_O to VDDS (voltage of stabilized power supply for the sensor interface) when the voltage of v_I is lower than V_T^-, and will change v_O to GND when the voltage of v_I is higher than V_T^+.

- So the circuit of Fig-14 will be analyzed to obtain $f(R_s)$, and then its inverse function $R_s(f) = R_{sensor}$ that is useful for using/configuring the Multiple-Sensor Interface. Notice that $I_i \approx 0$ since V_i is the input of the Schmitt-trigger inverter(high-speed Si-gate CMOS) that has a very high input impedance and so $I_i \approx 0$ is an appropriate approximation simplifying the circuit. So from the circuit are obtained the equations:

Nodes and loops: $i_4 = i_s + i_1$, $i_3 + i_s = i_2$, $i_o = i_3 + i_4$, $i_1 + i_2 = i_o$, $i_1 + i_2 = i_3 + i_4$, $v_1 - v_2 - v_s = 0$, $v_4 + v_s + v_2 - v_o = 0$, $v_4 + v_s - v_3 = 0$, $v_3 = v_o - v_2$, $v_4 = v_o - v_i$, $v_2 = v_i - v_s$.

Components: $i_1 = C_1(dv_1/dt)$, $i_2 = C_2(dv_2/dt)$, $v_3 = R_2 i_3$, $v_4 = R_1 i_4$, $v_s = R_s i_s$

Solving:

$$\frac{v_o - v_i}{R_1} = \frac{v_s}{R_s} + C_1 \frac{dv_i}{dt} \qquad (9)$$

$$\frac{v_o - v_i + v_s}{R_2} + \frac{v_s}{R_s} = C_2 \frac{dv_2}{dt} \qquad (10)$$

- Solving: $v_2 = v_i - v_s \Rightarrow dv_2/dt = d(v_i - v_s)/dt \Rightarrow dv_2/dt = (dv_i/dt) - (dv_s/dt)$

- So using the previous result the Eq-10 can be changed to:

$$\frac{v_o - v_i}{R_2} + \left(\frac{1}{R_2} + \frac{1}{R_s}\right) v_s = C_2 \left(\frac{dv_i}{dt} - \frac{v_s}{dt}\right) \qquad (11)$$

- Solving Eq-9 for v_s is obtained:

$$v_s = \frac{R_s(v_o - v_i)}{R_1} - R_s C_1 \frac{dv_i}{dt} \qquad (12)$$

- Calculating the derivative on both sides of Eq-12 is obtained (remember v_o is a constant equal to VDDS or GND depending on the position of the switch 'SW'):

$$\frac{dv_s}{dt} = \frac{-R_s}{R_1} \frac{dv_i}{dt} - R_s C_1 \frac{d^2 v_i}{dt^2} \qquad (13)$$

- Now using Eq-12 and Eq-13 to remove the variables v_s and dv_s/dt from the Eq-11 is obtained an equation solvable

6

for determining $v_i(t)$:

$$\left(\frac{1}{R_2} + \frac{R_s}{R_2 R_1} + \frac{1}{R_1}\right)(v_o - v_i) =$$

$$\left(C_1\left(1 + \frac{R_s}{R_2}\right) + C_2\left(1 + \frac{R_s}{R_1}\right)\right)\frac{dv_i}{dt} + R_s C_1 C_2 \frac{d^2 v_i}{dt^2}$$
(14)

- The Eq-14 is of the type: $c(v_o - v_i) = b(dv_i/dt) + a(d^2 v_i/dt^2)$ that has the general solution: $v_i(t) = v_o + k_1 e^{\lambda_1 t} + k_2 e^{\lambda_2 t}$, where k_1, k_2 are integration constants to be defined by 'initial conditions' and λ_1, λ_2 are defined by: $a\lambda^2 + b\lambda + c = 0 \Leftrightarrow \lambda = \frac{-b \pm \sqrt{b^2 - 4ac}}{2a}$ and e is the Euler-Napier constant $e = \sum_{n=0}^{\infty}(1/(n!))$.

- So for a solution to this circuit: $a = R_s C_1 C_2$,

$b = (C_1(1 + (R_s/R_2))) + (C_2(1 + (R_s/R_1)))$,

$c = (1/R_2) + (R_s/(R_2 R_1)) + (1/R_1)$.

- Is selected the solution of $\lambda_2 = \frac{-b + \sqrt{b^2 - 4ac}}{2a}$ by setting $K_1 = 0$, because is the one that will provide an adequate value for $v_i(t)$ and $f(R_s)$ consistent with experimental data, however for obtaining the function $R_s(f)$ you may use any.

- For convenience of making $v_i(t)$ more similar to typical RC circuits will be defined a new variable $\tau = -1/\lambda$ and so $v_i(t) = v_o + k_2 e^{-t/\tau_2}$.

- Charging time of C_1: $v_o = VDDS$
$v_i(t=0)=V_T^- \rightarrow V_T^- = VDDS + k_2 e^0 \rightarrow k_2 = V_T^- - VDDS$
$v_i(t=T_C)=V_T^+ \rightarrow V_T^+ = VDDS + k_2 e^{-T_C/\tau_2} \rightarrow$
$\rightarrow T_C = -\tau_2 ln((V_T^+ - VDDS)/(V_T^- - VDDS))$

- Discharging time of C_1: $v_o = 0$
$v_i(t=0)=V_T^+ \rightarrow V_T^+ = 0 + k_2 e^0 \rightarrow k_2 = V_T^+$
$v_i(t=T_D)=V_T^- \rightarrow V_T^- = 0 + k_2 e^{-T_D/\tau_2} \rightarrow$
$\rightarrow T_D = -\tau_2 ln(V_T^-/V_T^+)$

- The time for a complete cycle of charge and discharge of C_1 is: $T = T_C + T_D$; the frequency of $v_i(t)$ is $f = 1/T$.

- Solving: $T = -\tau_2\left(ln\left(\frac{V_T^+ - VDDS}{V_T^- - VDDS}\right) + ln\left(\frac{V_T^-}{V_T^+}\right)\right)$
$\Leftrightarrow T = \tau_2 ln\left(\frac{(V_T^- - VDDS)V_T^+}{(V_T^+ - VDDS)V_T^-}\right)$

- For convenience defining the constant 'H' by:
$$H = ln\left(\frac{(V_T^- - VDDS)V_T^+}{(V_T^+ - VDDS)V_T^-}\right),$$
then $f = 1/T \Leftrightarrow f = 1/(\tau_2 H) \Leftrightarrow f = -\lambda_2/H$.

- So the expression (theoretical) of measured resistance R_{sensor} as a function of frequency(f) is:
$$R_{sensor} = R_s = \frac{(C_1 + C_2)R_2 R_1 H f - R_2 - R_1}{(C_2 R_2 H f - 1)(C_1 R_1 H f - 1)} \quad (15)$$

- So using the values of $C_1=C_2=2.2nF$, $R_2=500\Omega$, $R_1=2M\Omega$, $V_T^-=1.2V$, $V_T^+=2.2V$, $VDDS=4.18V$, is obtained $H=1.01496$, Fig-15 shows experimental data for Multiple-Sensor Interface with various resistance values connected as the sensor and also shows the plot of $R_{sensor}(f)$ using Eq-15 with the mentioned values of C_1, C_2, R_2, R_1, H.
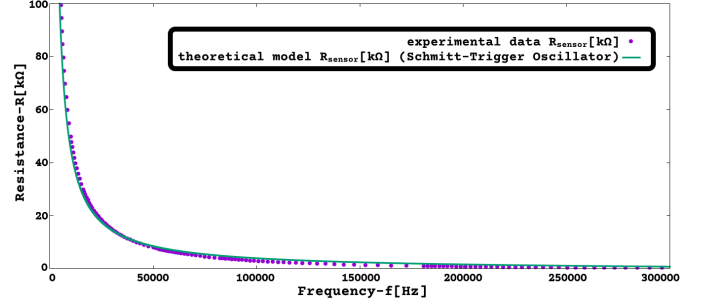

Figure 15: $R_s[k\Omega]$ versus frequency[0Hz, 300000Hz] (Schmitt-Trigger Oscillator, Multiple-Sensor Interface with resistive sensor).

4.3. Multiple-Sensor Interface for capacitive sensors

- In case you connect a capacitive sensor (or resistive) to the Multiple-Sensor Interface you will not be able to satisfy the conditions for oscillation (Eq-3 and Eq-4) were $A(\omega_0)\beta(\omega_0)=1$, and so for capacitive sensors again you no longer have a Pierce Oscillator, but instead have a Schmitt-trigger relaxation oscillator.

- So to analyze this circuit the Schmitt-trigger inverter will be replaced by a theoretical switch that will change the voltage of node v_O to VDDS (voltage of stabilized power supply for the sensor interface) when the voltage of v_I is lower than V_T^-, and will change v_O to GND when the voltage of v_I is higher than V_T^+.

- So the circuit of Fig-16 will be analyzed to obtain $f(C_s)$, and then its inverse function $C_s(f) = C_{sensor}$ that is useful for using/configuring the Multiple-Sensor Interface. Notice that $I_i \approx 0$ since V_i is the input of the Schmitt-trigger inverter(high-speed Si-gate CMOS) that has a very high input impedance and so $I_i \approx 0$ is an appropriate approximation simplifying the circuit. So from the circuit are obtained the equations:

Nodes and loops: $i_4 = i_s + i_1$, $\quad i_3 + i_s = i_2$, $i_o = i_3 + i_4$, $\quad i_1 + i_2 = i_o$, $\quad i_1 + i_2 = i_3 + i_4$, $v_1 - v_2 - v_s = 0$, $\quad v_4 + v_s + v_2 - v_o = 0$, $\quad v_4 + v_s - v_3 = 0$, $v_3 = v_o - v_2$, $\quad v_4 = v_o - v_i$, $\quad v_2 = v_i - v_s$.

Components: $i_1 = C_1(dv_1/dt)$, $\quad i_2 = C_2(dv_2/dt)$, $v_3 = R_2 i_3$, $\quad v_4 = R_1 i_4$, $\quad i_s = C_s(dv_s/dt)$

Solving:
$$\frac{v_o - v_i}{R_1} = C_s\frac{dv_s}{dt} + C_1\frac{dv_i}{dt} \quad (16)$$
$$\frac{v_o - v_2}{R_2} + C_s\frac{dv_s}{dt} = C_2\frac{dv_2}{dt} \quad (17)$$
$$\frac{v_o - v_2}{R_2} + \frac{v_o - v_i}{R_1} = C_1\frac{dv_i}{dt} + C_2\frac{dv_2}{dt} \quad (18)$$

- Since $v_s = v_i - v_2$ then $dv_s/dt = (dv_i/dt) - (dv_2/dt)$,
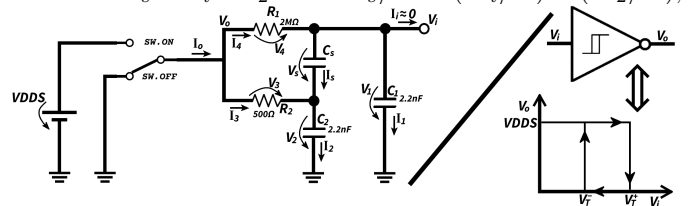

Figure 16: Multiple-Sensor Interface with capacitive sensor (Schmitt-trigger inverter oscillator).

and so using it on Eq-16 is obtained:

$$\frac{dv_2}{dt} = \left(1 + \frac{C_1}{C_s}\right)\frac{dv_i}{dt} - \frac{v_o - v_i}{C_s R_1} \qquad (19)$$

- Using $dv_s/dt = (dv_i/dt) - (dv_2/dt)$ and Eq-19 on Eq-17 is obtained:

$$v_2 = v_o + \frac{R_2(C_2 + C_s)(v_o - v_i)}{C_s R_1} + R_2 C_s\left(1 - \left(1 + \frac{C_2}{C_s}\right)\left(1 + \frac{C_1}{C_s}\right)\right)\frac{dv_i}{dt} \qquad (20)$$

- Calculating the derivative of Eq-20 is obtained:

$$\frac{d(v_2)}{dt} = -\frac{R_2(C_2 + C_s)}{C_s R_1}\frac{dv_i}{dt} + R_2 C_s\left(1 - \left(1 + \frac{C_2}{C_s}\right)\left(1 + \frac{C_1}{C_s}\right)\right)\frac{d^2 v_i}{dt^2} \qquad (21)$$

- Now using Eq-20 and Eq-21 to remove the variables v_2 and dv_2/dt from the Eq-18 is obtained an equation solvable for determining $v_i(t)$:

$$v_o - v_i = (R_2(C_2 + C_s) + R_1(C_1 + C_s))\frac{dv_i}{dt} + R_2 R_1(C_1 C_2 + C_s(C_1 + C_2))\frac{d^2 v_i}{dt^2} \qquad (22)$$

- The Eq-22 is of the type: $c(v_o - v_i) = b(dv_i/dt) + a(d^2 v_i/dt^2)$ that has the general solution:
$v_i(t) = v_o + k_1 e^{\lambda_1 t} + k_2 e^{\lambda_2 t}$, where k_1, k_2 are integration constants to be defined by 'initial conditions' and λ_1, λ_2 are defined by: $a\lambda^2 + b\lambda + c = 0 \Leftrightarrow \lambda = \frac{-b \pm \sqrt{b^2 - 4ac}}{2a}$ and e is the Euler-Napier constant $e = \sum_{n=0}^{\infty}(1/(n!))$.
- So for a solution to this circuit: $c = 1$,
$b = (R_2(C_2 + C_s) + R_1(C_1 + C_s))$,
$a = R_2 R_1(C_1 C_2 + C_s(C_1 + C_2))$.
- Is selected the solution of $\lambda_2 = \frac{-b + \sqrt{b^2 - 4ac}}{2a}$ by setting $K_1 = 0$, because is the one that will provide an adequate value for $v_i(t)$ and $f(C_s)$ consistent with experimental data, however for obtaining the function $C_s(f)$ you may use any.
- For convenience of making $v_i(t)$ more similar to typical RC circuits will be defined a new variable $\tau = -1/\lambda$ and so $v_i(t) = v_o + k_2 e^{-t/\tau_2}$.

- So when is connected a capacitive sensor (C_s) the differential equation and solution $v_i(t)$ are the same as when is connected a resistive sensor (R_s), the only differences are on the values of a, b, c; and as such the equations of f(frequency) and T(period) are also the same and will be reused from the previous chapter.
- The constant 'H' defined by:

$$H = ln\left(\frac{(V_T^- - VDDS)V_T^+}{(V_T^+ - VDDS)V_T^-}\right),$$

and $f = 1/T \Leftrightarrow f = 1/(\tau_2 H) \Leftrightarrow f = -\lambda_2/H$.
- So the expression (theoretical) of measured Capacitance C_{sensor} as a function of frequency(f) is:

$$C_{sensor} = C_s = \frac{(C_1 R_1 + C_2 R_2)Hf - 1 - C_1 C_2 R_1 R_2 H^2 f^2}{Hf((C_1 + C_2)R_1 R_2 Hf - R_1 - R_2)} \qquad (23)$$

- So using the values $VDDS=4.18V$, $C_1=C_2=2.2nF$, $R_1=2M\Omega$, $R_2=500\Omega$, $V_T^-=1.2V$, $V_T^+=2.2V$ is obtained $H=1.01496$, and Fig-17 shows the plot of $C_{sensor}(f)$ using Eq-23 with the mentioned values of C_1, C_2, R_2, R_1, H.
- Analyzing the plot on Fig-17 by firstly looking at plot regions with $C_s > 0$, its visible that the $C_s(f)$ plot is over the C_s axis (this is the vertical axis f=0) and this would mean that for all values of C_s the frequency would be zero
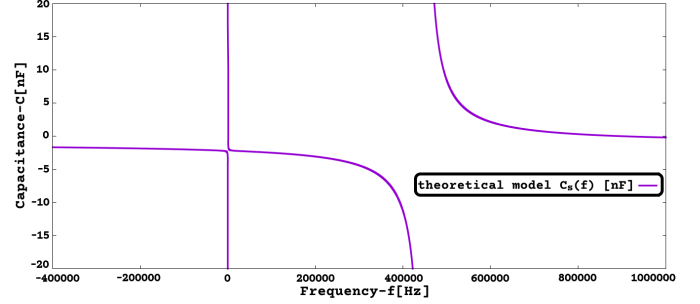

Figure 17: $C_s(f)$ [nF] versus frequency[-400kHz, 1MHz] (Schmitt-Trigger Oscillator, Multiple-Sensor Interface with capacitive sensor). (f=0), but also visible to the right is another curve that is also placed on the area of $C_s > 0$ (for frequency[447957Hz, 895689Hz]) and at first this curve would be expected to define the operating frequency of the oscillator depending on the capacitance of the connected sensor.

- However experimental data will show that the way the oscillator works using a capacitive sensor is very different from what would be expected from a first view on the plot of function $C_s(f)$, in order to compare the experimental data with the theoretical model is shown on Fig-18 and Fig-19 the experimental data for Multiple-Sensor Interface with various capacitance values connected as the sensor and also the plot of $abs(C_s(f))$ $(= |C_s(f)|)$ using Eq-23 with the mentioned values of C_1, C_2, R_1, R_2, H.

- So it seems that the obtained function of $C_s(f)$ although strangely indicates negative values for the sensor capacitance it can provide a theoretical curve/plot very similar to what was obtained on the experimental data for C_{sensor}. On the following chapters will be given a better insight on why $C_s(f)$ has a negative value.
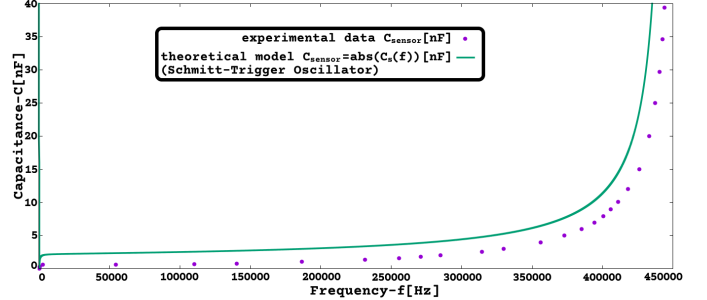

Figure 18: C_s[nF] versus frequency[0Hz, 440000Hz] by $|C_s(f)|$ (Schmitt-Trigger Oscillator, Multiple-Sensor Int. with capacitive sensor).
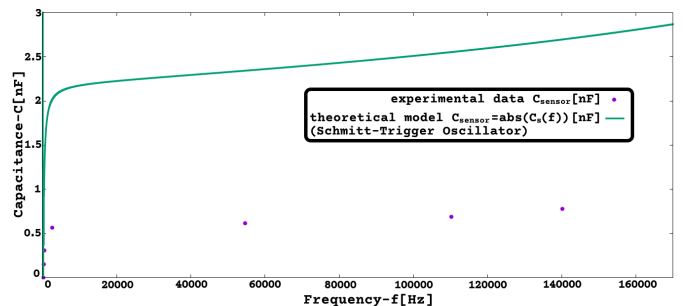

Figure 19: C_s[nF] versus frequency[0Hz, 170000Hz] by $|C_s(f)|$ (Schmitt-Trigger Oscillator, Multiple-Sensor Int. with capacitive sensor).

8

4.4. Multiple-Sensor Int. for measuring frequency

- For measuring frequency of an external voltage signal (between 0V and VDDS, so preferentially a digital signal or in case of analog signal it should be limited/trimmed before) is possible to use the mentioned Multiple-Sensor Interface and so using the same port/connector of the device. For this the user should remove/open the jumpers "JP.A", "JP.B" making the capacitors C1-A, C2-B active on the circuit, this will make $C_1 = C_2 = 21.8pF$ that is a quite low capacitance that will have an insignificant effect on the external voltage signal. The external voltage signal should be connected to the 1st pin of the sensor channel that is the one connected directly to input of the Schmitt-Trigger Inverter, so making the inverter directly driven by the external voltage signal, then the Multiple-Sensor Interface is just a converter of the voltage signal to a square wave signal where its frequency will be measured through the counter/timer of the PIC18F2550.

- The external voltage signal would preferentially be from a sensor with a square wave output, and the sensor have its power supplied by one of the VDD,GND ports/connectors of the Multiple-Sensor Interface device or by an external connection to the same power supply used to power the device.

5. Alternative Approximate Circuit Analysis

5.1. Sensor interface circuit simplified (for C_s or R_s)

- The Multiple-Sensor Interface circuit (oscillator) when using a capacitive or resistive sensor can be studied and understood in a more intuitive way by making some simplification/approximation that may be inaccurate for quantitative purposes but still captures its essence, with the benefit of exposing how it works and resulting in much simpler differential equations. So when using a capacitive or resistive sensor the circuit is a Schmitt-Trigger oscillator with a more complex circuit but its essence is the same, it is just some capacitors being charged by currents that pass trough some resistors, and the voltage on a capacitor(v_i) will trigger(at V_T^- or V_T^+) a switch(electronic inverter) to change the voltage(v_o).[3]

- So the proposed simplification/approximation (for C_s or R_s) is to admit the sensor and interface circuit can be described approximately by using the circuit of a basic/normal Schmitt-Trigger Oscillator that only has one capacitor and one resistor (that determine the frequency of oscillation), and so will be used the simplified circuit on Fig-20 where C_{approx} is a capacitor and R_{approx} is a resistor that approximate in overall the capacitance and resistance respectively of the sensor interface oscillator.

- To build expressions of C_{approx} and R_{approx} as a function of R_1, R_2, C_1; C_2 will be considered initially 2 extreme cases of the sensor impedance(Z_s): 1st $|Z_s|=0$ the sensor can be replaced by a wire, and 2nd $|Z_s|=\infty$ the sensor can be removed(open circuit), these 2 extreme cases possible for the sensor impedance are represented on Fig-21 .

- Now the sensor can be described as an electric connection that can be weakened or intensified depending on the
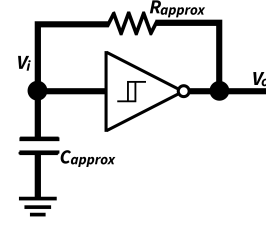

Figure 20: Schematic of a basic/normal Schmitt-Trigger Oscillator to be used as an approximation of the circuit of Multiple-Sensor Interface with capacitive or resistive sensor).
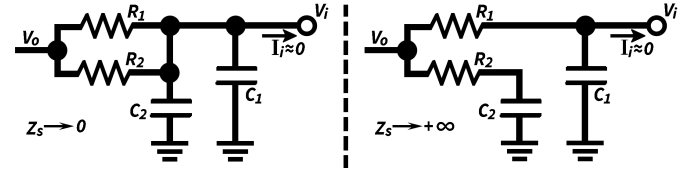

Figure 21: Schematic of the RC network of the Schmitt-Trigger Oscillator for the 2 extreme cases of the sensor impedance (Z_s).

sensor impedance, so when $|Z_s|$ changes progressively from 0 to $+\infty$ the circuit changes progressively and smoothly from the left circuit to the right circuit on Fig-21. So to obtain equations for R_{approx} and C_{approx} will be selected an expression that allows to change smoothly the resistance and capacitance of the RC circuit on the left side of (Fig-21) to the resistance and capacitance of the RC circuit on the right side of (Fig-21).

- So as on Fig-21, here are the values of C_{approx} and R_{approx} for the 2 extreme values of $|Z_s|=0$ and $|Z_s|=+\infty$:
$C_{approx}(Z_s{=}0){=}C_1{+}C_2$; $C_{approx}(Z_s{=}\infty){=}C_1$;
$R_{approx}(Z_s{=}0){=}(R_1 R_2)/(R_1{+}R_2)$; $R_{approx}(Z_s{=}\infty){=}R_1$;

5.1.1. R_{approx} and C_{approx} for a resisitve sensor (R_s)

Here are functions modeled to describe C_{approx} and R_{approx} (with resistive sensor) with a smooth transition from its values at $|Z_s|=0$ and $|Z_s|=+\infty$, where $|Z_s|=R_s$:

$$C_{approx} = (C_1 + C_2)\frac{R_1}{|Z_s| + R_1} + C_1\frac{|Z_s|}{|Z_s| + R_1} \qquad (24)$$

$$R_{approx} = \frac{R_1 R_2}{R_1 + R_2}\frac{2R_1}{|Z_s| + 2R_1} + R_1\frac{|Z_s|}{|Z_s| + 2R_1} \qquad (25)$$

Using the equations: $f = 1/T \Leftrightarrow f = 1/(\tau_2 H) \Leftrightarrow f = -\lambda_2/H$; and using $\tau_2 = R_{approx}C_{approx}$ can be obtained $f(R_s)$ and/or $R_s(f)$.

- So using the values of $C_1{=}C_2{=}2.2nF$, $R_2{=}500\Omega$, $R_1{=}2M\Omega$, $V_T^-{=}1.2V$, $V_T^+{=}2.2V$, $VDDS{=}4.18V$, is obtained $H{=}1.01496$, and Fig-22 shows the plot of $R_s(f)$ using the approximate model (C_{approx}, R_{approx}) with the mentioned values of C_1, C_2, R_2, R_1, H.

5.1.2. R_{approx} and C_{approx} for a capacitive sensor (C_s)

Here are functions modeled to describe C_{approx} and R_{approx} (with capacitive sensor) with a smooth transition from its values at $|Z_s|=0$ and $|Z_s|=+\infty$, where $|Z_s|=1/(2\pi f C_s)$:

$$C_{approx} = (C_1 + C_2)\frac{R_1}{|Z_s| + R_1} + C_1\frac{|Z_s|}{|Z_s| + R_1} \qquad (26)$$

$$R_{approx} = \frac{R_1 R_2}{R_1 + R_2}\frac{R_1}{|Z_s| + R_1} + R_1\frac{|Z_s|}{|Z_s| + R_1} \qquad (27)$$
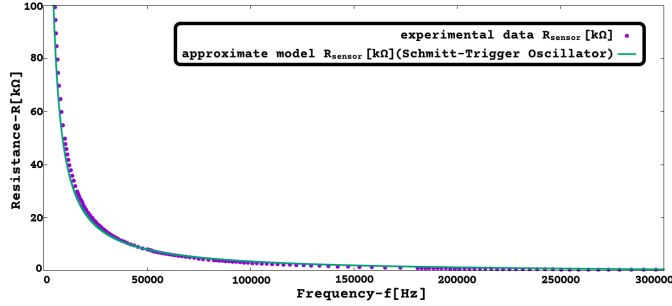
9

Figure 22: $R_s(f)[\mathrm{k\Omega}]([\mathrm{Hz}])$ by approximate model (C_{approx}, R_{approx}; Multiple-Sensor Int. with resistive sensor).
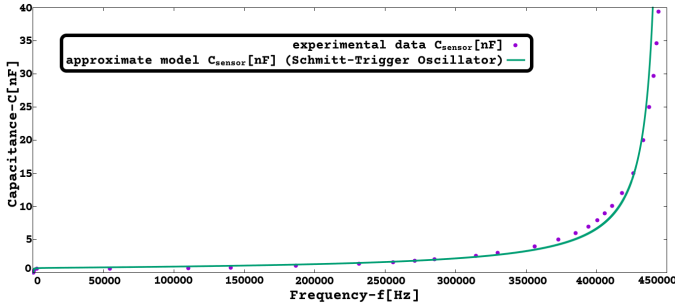

Figure 23: $C_s[\mathrm{nF}]$ versus frequency[0Hz, 450kHz] by approximate model (C_{approx}, R_{approx}; Multiple-Sensor with capacitive sensor).
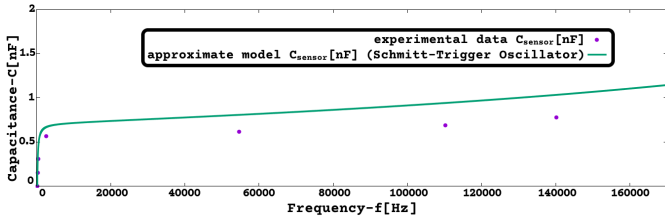

Figure 24: $C_s[\mathrm{nF}]$ versus frequency[0Hz, 170kHz] by approximate model (C_{approx}, R_{approx}; Multiple-Sensor with capacitive sensor).

- So using the values of $C_1{=}C_2{=}2.2nF$, $R_2{=}500\Omega$, $R_1{=}2M\Omega$, $V_T^-{=}1.2V$, $V_T^+{=}2.2V$, $VDDS{=}4.18V$, is obtained $H{=}1.01496$, and Fig-23 and Fig-24 shows the plot of $C_s(f)$ using the approximate model (C_{approx}, R_{approx}) with the mentioned values of C_1, C_2, R_2, R_1, H.

5.2. Why $C_s(f){<}0$ on Multi-Sensor with capacitive sensor

- About $C_s(f) < 0$ have in mind the Multiple-Sensor with a capacitive sensor is studied on transient behavior (relaxation oscillator), where 'frequency' is a measure of the speed of charge and discharge on C1; and also of how fast the transient circuit analysis alternates between 2 different schematics ($v_o = VDDS$ and $v_o = 0$).

- To understand why a normal capacitor behaves as negative capacitance when connected as the sensor of the Multiple-Sensor Interface (this is, why $C_s(f) < 0$), is important to highlight some things already explored on the previous chapters: 1) $C_1{=}C_2$, $R_1 \gg R_2$;

2) The primary path (always available) to charge C_1 is through R_1, the primary path (always available) to charge C_2 is through R_2, since $R_1 \gg R_2$ and $C_1{=}C_2$ this implies that capacitor C_2 will charge/discharge much faster(takes less time) than capacitor C_1.

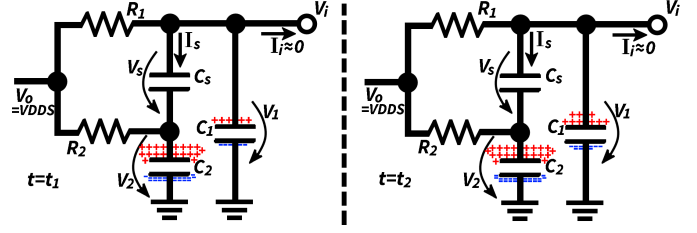3) The purpose of sensor C_s on this circuit is to act as a

Figure 25: Schematic of RC network of the Schmitt-Trigger Oscillator with a representation of electrical charge on C_1 and C_2 on $t{=}t_1$ and $t{=}t_2$.

variable impedance that can establish an alternative path on the circuit ($V_o \to R_2 \to C_s \to C_1$) to charge/discharge capacitor C_1; so $C_s \nearrow \Rightarrow |Z_s| \searrow \Rightarrow R_{approx} \searrow \Rightarrow \tau_2 \searrow \Rightarrow$ C_1charges faster;

4) No matter how small $|Z_s|$ may be the capacitor C_2 will always charge/discharge faster than capacitor C_1, and on the limit where $|Z_s|{=}0$ the capacitors C_1 and C_2 will be charged/discharged simultaneously.

- For the following discussion will be used as definition of capacitance the formula $C_s = i_s/(dv_s/dt)$, where the $|C_s| = |Q_s|/|v_s|$ (C_s: [F] farad; Q_s: [C] coulomb; v_s [V] volt), and since the only purpose is to show how C_s can be a negative number it will be used the approximate expression $C_s \approx \overline{i_s}/(\Delta v_s/\Delta t)$ that will provide exactly the same sign as the exact formula.

- To show is possible $C_s < 0$ will be considered qualitative relations of the circuit electrical parameters on the RC network of the oscillator, the relevant electrical parameters and their variation between $t{=}t_1$ and $t{=}t_2$ is represented on Fig-25 .

- It will be assumed symbolic values for the voltages on the circuit, used as specimen values to determine how fast a voltage is changing between t_1 and t_2 time moments. So for representing a small amount of electrical charge will be used the symbols: [+] for positive charge and [-] for negative charge, since already stated $C_1 = C_2$ for each additional amount of [+] and [-] charge stored on each plate (of C_1 or C_2) will cause an increase of capacitor voltage that will be represented as $[+\underline{v}]$, where $C_1 = C_2 = [+]/[+\underline{v}]$.

- As visible on Fig-25 $V_o{=}VDDS \approx +4.18V$, and so $VDDS$ will eventually be the voltage on C_1 and C_2 when $t \to \infty$. For making visual on the schematic the charging process, the charge accumulated in C_1, C_2 was divided in 20 sets, each represented by [+], [-]; and for each set of accumulated charge is associated a corresponding increase in voltage of $[+\underline{v}]$, and so $[+\underline{v}] = VDDS/20$.

- Accordingly on Fig-25 is represented that C_2 is charged to near the final value ($VDDS$) during the interval $[0;t_1]$ while C_1 charges much slower. During interval $[t_1;t_2]$ is visible that C_2 increased its charge only by 1[+] becoming charged to approximately(or practically) its final value($v_2 \approx VDDS$), whether C_1 is still charging and v_1 is far from its final value($VDDS$), but interestingly v_1 is now increasing faster than v_2, because v_2 already reached its final value, this is $dv_1/dt > dv_2/dt, \forall t \in [t_1;t_2]$. The specimen values here mentioned are in line with the exponential function typical of capacitors charging through a resistor,

10

where lets say a capacitor initially charges very fast, when has some charge stored it charges more slowly, and when close to being full it charges very slowly (where full means the capacitor voltage is close to power supply voltage).

5.2.1. Voltage and current specimens for $t=t_1$

- So looking at the schematic on left side of Fig-25 is visible C_1 and C_2 are charging and for $t=t_1$ the charge on C_1 is 19[+] and on C_2 is 5[+], so capacitor C_2 is almost charged while C_1 is still charging. The capacitor C_1 is charging through the path $V_o \rightarrow R_1 \rightarrow C_1$ but mainly is charging through path $V_o \rightarrow R_2 \rightarrow C_s \rightarrow C_1$ and since $v_2 > v_1$ then $i_s(t=t_1) < 0$.

- For $t=t_1$ since Q_1=5[+] and Q_2=19[+] then v_1=5[+$\underline{v}$] and v_2=19[+$\underline{v}$], since $v_s = v_1 - v_2$ then $v_s(t=t_1) = 5[+\underline{v}] - 19[+\underline{v}] = -14[+\underline{v}]$.

5.2.2. Voltage and current specimens for $t=t_2$

- So looking at the schematic on right side of Fig-25 is visible C_1 and C_2 are charging and for $t=t_2$ the charge on C_1 is 20[+] and on C_2 is 9[+], so capacitor C_2 is fully charged while C_1 is still charging. The capacitor C_1 is charging through the path $V_o \rightarrow R_1 \rightarrow C_1$ but mainly is charging through path $V_o \rightarrow R_2 \rightarrow C_s \rightarrow C_1$ and since $v_2 > v_1$ then $i_s(t=t_2) < 0$.

- For $t=t_2$ since Q_1=9[+] and Q_2=20[+] then v_1=9[+$\underline{v}$] and v_2=20[+$\underline{v}$], since $v_s = v_1 - v_2$ then $v_s(t=t_2) = 9[+\underline{v}] - 20[+\underline{v}] = -11[+\underline{v}]$.

5.2.3. Sign of C_s as calculated from v_s and i_s during $[t_1; t_2]$

- The schematics on Fig-25 refer to a charging cycle of the Schmitt Trigger Oscillator. Also $t_2 > t_1 \rightarrow \Delta t > 0$.

- For $t \in [t_1; t_2]$ the capacitor C_1 is being charged through the path $V_o \rightarrow R_2 \rightarrow C_s \rightarrow C_1$ and so $i_s(t) < 0, \forall t \in [t_1; t_2] \Rightarrow \overline{i_s} < 0$.

- Also Δv_s between t_1 and t_2 is $\Delta v_s = v_s(t=t_2) - v_s(t=t_1) = -11[+\underline{v}] - (-14[+\underline{v}]) = 3[+\underline{v}]$, and so $\Delta v_s > 0$ between t_1 and t_2.

- So concluding between t_1 and t_2, $\Delta t > 0$, $\Delta v_s > 0$, $\overline{i_s} < 0 \Rightarrow C_s < 0$ accordingly with $C_s \approx \overline{i_s}/(\Delta v_s/\Delta t)$.

5.3. Comparison to known cases of negative capacitance

- Aspects of Multiple Sensor Interface circuit possibly related to negative capacitance phenomenon:
1- Use of Schmitt-Trigger 'NOT' gate which exhibits hysteresis on its $v_o(v_i)$ graph.
2- Multiple Sensor Interface with a capacitive sensor operates under transient(time domain) step voltage changes, caused by its 'NOT' gate(Schmitt-Trigger) alternating between 0V and +VDDS (relaxation oscillator).

- Negative capacitance phenomenon is reported on some scientific articles/texts, and interestingly with some coincidence to the 2 aspects mentioned above. Quotes:
1- "Effective negative capacitance has been postulated in ferroelectrics because there is hysteresis in plots of polarization-electric field.", article "Towards steep slope MOSFETs using ferroelectric negative capacitance", year 2014 [4].

2- "The phenomenon of negative capacitance, which has been reported in a variety of situations involving electrolytic as well as electronic systems, ... It is suggested that the physically correct approach lies in the analysis of the corresponding time-domain behavior under step function bias, which involves a current initially falling and then rising gradually over a period of time before finally decaying to zero.", article "The physical origin of negative capacitance", year 1986 [5].

Declaration of competing interest
None.

Appendix A. Experimental Datasets

Here is made available subsets (small list) of experimental data with measured values of Inductance, Resistance, Capacitance paired with measured frequency on the Multiple Sensor Interface device. Is made available only a limited subset of the experimental data that was used for drawing the plots of $L_s(f)$, $R_s(f)$, $C_s(f)$ for reference purposes, since placing here the full dataset would make the article exceedingly long. On the tests were used arrays(PCBs) with inductor, resistor, capacitor that allow to obtain various different values just by changing a jumper/switch, also were used single components (including in series or parallel association); these fixed value components were connected as the sensor on the device.

Appendix A.1. Frequency measurement by Multi-Sensor

- The Multiple-Sensor device measures frequency using a counter inside the microcontroller and has some accuracy and range limitations, the device can measure up to 3MHz (higher frequency causes counter overflow). The device was tested with a square wave signal from signal generator JDS6600 (by Joy-IT, frequency accuracy: ±20ppm).

- The Multiple-Sensor device measurement accuracy (percentage error) of frequency, is worst at low frequencies with 9% error at 100Hz and 0.7% error at 1kHz, above 5kHz the error was always smaller than 0.2% (ignoring any accuracy error by JDS6600 used as reference). The Multiple-Sensor device measurement precision (variation) for frequency was worst at low frequencies with 5% variation at 300Hz, above 1500Hz was always smaller than 1%, and above 15kHz was always smaller than 0.1%.

Appendix A.2. Experimental data of Multiple-Sensor

Here are subset (some pairs) of measured experimental data for $L_s(f)$, $R_S(f)$, $C_s(f)$.
- **Jumper Configurations:**
  [a](JPA on, JPB off): C_1=2.2nF; C_2=21.8pF.
  [b](JPA off, JPB on): C_1=21.8pF; C_2=2.2nF.
  [c](JPA on, JPB on): C_1=2.2nF; C_2=2.2nF .
- **Units:** Hz=hertz, H=henry, Ω=ohm, F=farad.

- **Reference instruments:** The measurements of inductance(L_s) and capacitance(C_s) were obtained using the LCR meter TH2821A (by Tonghui, basic accuracy

0.3%), configured to 10Khz test signal. The measurements of resistance(R_s) were obtained using the meter UT603 (by UNI-T, accuracy: 0.8% for R≤2MΩ; 2% for R>2MΩ;).

Table A.1: Subset of experimental data for $L_s(f)$

$L_s[\mu H]$ Inductance	f[Hz][a] JPA on, JPB off	f[Hz][b] JPA off, JPB on	f[Hz][c] JPA on, JPB on
1.21	834161	879205	446590
1.85	833014	887049	458577
4.7	826011	881239	496405
9.7	813397	858548	615743
11.77	808321	936894	1432920
15.76	799009	895932	1251070
21.39	785691	931940	1090760
31.8	760632	1056660	889633
46.7	726580	1369450	736014
53.44	712070	2853370	690970
95.34	620697	2103380	509845
173.5	502398	1575330	382571
341.8	368641	1112820	271168
558.1	287880	868105	212362
777.6	241031	737803	178480
921.2	218738	677591	163587
1491	161768	606844	124338
2171	130897	499264	102978
3170	105439	406011	84614
3640	97779	383305	79110
4646	84110	319423	69783
6880	68162	282360	57750
10140	54034	224090	47230
15040	43377	192088	38790
20375	36588	171981	33683

Precision error(maximum frequency variation):
±2kHz (high frequency); ±300Hz (low frequency);
±5kHz (2.85MHz↔1.36MHz; at [b] JPA off, JPB on)

Table A.2: Set of experimental data for $C_s(f)$

C_s[nF] Capacitance	f[Hz][c] JPA on, JPB on	C_s[nF] Capacitance	f[Hz][c] JPA on, JPB on
0	229	3.98	356012
0.152	321	4.97	373045
0.31	458	5.97	385032
0.568	2614	6.95	394283
0.615	54570	7.94	400750
0.689	110286	8.98	405766
0.776	140178	10.07	411246
1.015	186522	12.04	418028
1.34	231460	15.02	426040
1.58	255526	20.02	433089
1.79	271015	24.97	437446
2	285020	29.68	440382
2.56	314530	34.62	442584
2.99	329820	39.43	444235

Precision error(maximum frequency variation):
±3kHz (600pF<C_s<1.6nF); ±2kHz (1.6nF<C_s<21nF);
±1kHz (C_s>21nF); ±50Hz (C_s<600pF).

Table A.3: Subset of experimental data for $R_s(f)$

$R_s[\Omega]$ Resistance	f[Hz][c] JPA on, JPB on	$R_s[\Omega]$ Resistance	f[Hz][c] JPA on, JPB on
0	456284	6970	55288
1.2	454678	9960	41879
5.2	451605	14950	29861
10.2	447385	19940	23271
20.1	439144	24900	19066
50	416407	29900	16176
99.9	383396	39800	16176
139.7	361700	49800	10091
199.5	333306	69700	7385
299	296289	99400	5320
398	268278	149300	3623
498	246214	199100	2798
697	213647	299000	1972
996	180865	498000	1284
1494	147150	697000	978
1992	125699	995000	779
2990	98819	1993000	504
3980	82153	5080000	351
4980	70593	9040000	305

Precision error(maximum frequency variation):
±1kHz (high freq); ±300Hz (at 30kΩ); ±100Hz (low freq).

References

[1] Jaeger, R.C.; Blalock, T.N. (2011). Microelectronic Circuit Design (4rd ed.). McGraw–Hill. ISBN 978-0-07-338045-2. - "C.2 THE HYBRID OR h-PARAMETERS - Appendix C Two-Port Review" - Pag.1310-1311 . *Alternative Source: "Hybrid parameters (h-parameters) - Two-port Network - Wikipedia (2020)"* - `https://en.wikipedia.org/wiki/Two-port_network`

[2] Peter McLean (2020) - Topic 4 - Crystal Oscillators (Analysis of the Pierce oscillator) - Digital Electronics (UTS-AU) - `https://pmcl.net.au/de/`

[3] Eduardo Corpeno (2018) - Exactly How Schmitt Trigger Oscillators Work - AllAboutCircuits - `https://www.allaboutcircuits.com/technical-articles/exactly-how-schmitt-trigger-oscillators-work`

[4] O'Neill, A and Appleby, D and Ponon, N and Kwa, K (2014). Towards steep slope MOSFETs using ferroelectric negative capacitance. 2014 12th IEEE International Conference on Solid-State and Integrated Circuit Technology (ICSICT). DOI: 10.1109/ICSICT.2014.7021281 .

[5] Jonscher, Andrew K. (1986). The physical origin of negative capacitance. J. Chem. Soc., Faraday Trans. 2, vol. 82, no. 1, Pag.75-81. DOI: 10.1039/F29868200075 .

[6] Thomas Williams, Colin Kelley (2007) - GNUplot software - For drawing the plots/graph - `http://gnuplot.sourceforge.net`